

Research Article

On the Elevated Temperature, Tensile Properties of Al-Cu Cast Alloys: Role of Heat Treatment

A. Girgis,¹ A. M. Samuel,¹ H. W. Doty,² S. Valtierra,³ and F. H. Samuel ¹

¹Département des Sciences Appliquées, Université du Québec à Chicoutimi, Chicoutimi, QC, Canada

²General Motors Materials Engineering, 823 Joslyn Ave, Pontiac, MI 48340, USA

³Nemak S. A., P.O. Box 100, Garza Garcia, NL 66221, Mexico

Correspondence should be addressed to F. H. Samuel; fhsamuel@uqac.ca

Received 24 June 2019; Accepted 13 November 2019; Published 13 December 2019

Academic Editor: Lingxue Kong

Copyright © 2019 A. Girgis et al. This is an open access article distributed under the Creative Commons Attribution License, which permits unrestricted use, distribution, and reproduction in any medium, provided the original work is properly cited.

The present study aims to investigate the mechanical properties of a newly developed aluminum Al-6.5% Cu-based alloy, coded HT200, as well as to determine how these properties can be further improved using grain refinement and heat treatment. As a result, the effects of different heat treatments and alloying additions on the ambient and high-temperature tensile properties were examined. Three alloys were selected for this study: (i) the base HT200 alloy (coded A), (ii) the base HT200 alloy containing 0.15% Ti + 0.15% Zr (coded B), and (iii) the base HT200 alloy containing 0.15% Ti + 0.15% Zr + 0.5%Ag (coded C). The properties of the three HT200 alloys were compared with those of 319 and 356 alloys (coded D and E, respectively), subjected to the same heat treatment conditions. The results obtained show the optimum high-temperature tensile properties and Q-values for the five alloys of interest, along with the corresponding heat treatment conditions associated with these properties. It was found that the T6 heat-treated alloy B was the optimum alloy in terms of properties obtained, with values comparable to those of commercial B319.0 and A356.0 alloys.

1. Introduction

The mechanical properties of aluminum-copper casting alloys can be improved through an appropriate control of the different metallurgical parameters involved in the production of these castings. Some alloying elements can be used as grain refiners which improve the mechanical properties, reduce ingot cracking, and give better mechanical deformation characteristics. Particles can be added into the melt in the form of master alloys that will nucleate new crystals during solidification [1]. This technique can be used in combination with heat treatment to further improve the mechanical properties of aluminum alloys [2]. Alloying elements affect the properties of aluminum alloys in different ways. For example, if hard, nonductile particles of a second phase are formed, strong barriers to dislocation motion are produced. Edge dislocations are repelled by such particles and screw dislocations have difficulty in bypassing them [3]. The characteristics of the alloying elements that were used in this

research study and their effects on aluminum alloys are presented here.

When the copper content is close to or above its solubility limit and the alloy is heat-treated so that the Cu is distributed in the GP zones, it gives the best combination of strength and ductility, as the precipitation of the second-phase θ contributes to the strengthening effect. The presence of a brittle network of eutectics (mostly Al-Al₂Cu) causes impact resistance, notch toughness, and fatigue resistance to decrease. On the other hand, strength at high temperature and resistance to creep and wear increase with increasing Cu content [4, 5]. Zirconium (Zr) is generally contained in aluminum alloys in amounts from 0.1 to 0.3 wt% and is used as a grain refiner, as it reduces the as-cast grain size which improves strength and ductility [3]. Zirconium is also added to form fine coherent precipitates of Al₃Zr (dispersoids). The hardening effect of Zr is attributed to the precipitation of the coherent coarsening-resistant Al₃Zr dispersoids during solution heat treatment [3, 6].

The *quality* of aluminum alloy castings may be defined using numerical values which correlate their mechanical properties [7]. The quality index, Q, and the probable yield strength, PYS, for aluminum casting alloys were developed empirically by Drouzy et al. [4, 8, 9].

In a previous article, the authors documented the microstructure, hot tearing, and tensile properties at ambient temperature of the same alloys [10]. As mentioned earlier, the present study was undertaken to investigate the mechanical properties of the HT200 alloy (alloy A) and to determine how these properties could be further improved using grain refinement and heat treatment. The main task was to optimize the alloy composition and heat treatment conditions to provide optimum properties at elevated temperatures and to compare them with the widely used B319.0 and A356.0 alloys to determine its suitability as a good alternative.

2. Experimental Procedure

The chemical composition of the base alloy HT200 is shown in Table 1. Two other alloys were prepared from this alloy, using additions of 0.15 wt% Ti + 0.15 wt% Zr, and 0.15 wt% Ti + 0.15 wt% Zr + 0.5 wt% Ag. These additions were made using Al-5% Ti-1% B and Al-15% Zr master alloys, while Ag was added in pure metal form. For the A319 alloy, 0.10 wt% Ti and 200 ppm Sr were added using Al-5% Ti-1% B and Al-10% Sr master alloys, respectively. The five alloys were coded A, B, C, D, and E as shown in Table 2. The as-received alloys were nongrain refined and unmodified. Boron content could not be determined with accuracy.

The HT200 base alloy was received in the form of small ingots. These ingots were melted in a 40 kg capacity SiC crucible using an electrical resistance furnace equipped with a rotary degassing impeller. The melting temperature was maintained at $800^{\circ}\text{C} \pm 5^{\circ}\text{C}$. In all cases, fluidity of the molten alloy was measured using a Ragone fluidity tester, model 4210, applying an overhead pressure of 200 mm Hg. For this purpose, glass tubes (140 cm long and 6 mm internal diameter) were used. The fluidity of pure aluminium was also measured for comparison. The tubes were preheated at 200°C before testing, and for each alloy, five consecutive fluidity tests were performed.

The melt was poured into an ASTM B-108 permanent mold preheated to 450°C (to drive out any moisture) in order to prepare test bars for tensile testing (cooling rate $7^{\circ}\text{C}/\text{s}$). Two standard tensile test bars were obtained for each casting. The standard tensile test bar has a gauge length of 70 mm and a cross-sectional diameter of 12.8 mm. Following the casting process, the tensile test bars were divided into bundles of five bars each. The as-cast bars were subjected to different heat treatments to enhance their mechanical properties. The various heat treatments used for this study were as follows:

- (1) As-cast
- (2) SHT* for 4 h followed by air quenching
- (3) SHT for 4 h followed by water quenching

- (4) SHT for 4 h followed by water quenching, then artificial aging 1 ($180^{\circ}\text{C}/4\text{ h}$)
- (5) SHT for 4 h followed by water quenching, then artificial aging 2 ($200^{\circ}\text{C}/4\text{ h}$)
- (6) SHT for 4 h followed by water quenching, then artificial aging 3 ($250^{\circ}\text{C}/4\text{ h}$)
- (7) SHT for 4 h followed by water quenching, then artificial aging 4 ($250^{\circ}\text{C}/100\text{ h}$)
- (8) SHT for 8 h followed by air quenching
- (9) SHT for 8 h followed by water quenching
- (10) SHT for 8 h followed by water quenching, then artificial aging 1 ($180^{\circ}\text{C}/4\text{ h}$)
- (11) SHT for 8 h followed by water quenching, then artificial aging 2 ($200^{\circ}\text{C}/4\text{ h}$)
- (12) SHT for 8 h followed by water quenching, then artificial aging 3 ($250^{\circ}\text{C}/4\text{ h}$)
- (13) SHT for 8 h followed by water quenching, then artificial aging 4 ($250^{\circ}\text{C}/100\text{ h}$)

* All solution heat treatments (SHT) for alloys A, B, and C were carried out at 520°C

* All solution heat treatments (SHT) for alloy D were carried out at $500^{\circ}\text{C}/8\text{ h}$

* All solution heat treatments (SHT) for alloy E were carried out at $540^{\circ}\text{C}/8\text{ h}$

Water quenching was done using warm water ($\sim 70^{\circ}\text{C}$).

Tensile testing at elevated temperature (250°C) was carried out employing an air forced Instron Universal Mechanical Testing machine, at a strain rate of $4 \times 10^{-4}\text{ s}^{-1}$. A K-type thermocouple was attached to the center of the tensile bar. The sample to be tested was mounted in the heated testing chamber and left for thirty minutes before starting the test in order to ensure a homogeneous distribution of the temperature throughout the sample. A data acquisition system attached to the machine provided readings of the ultimate tensile strength (UTS), the yield strength at 0.2% offset strain (YS), and the percentage elongation to fracture (%EL). In each case, 5–10 tensile bars were tested to achieve standard deviation of $\pm 5\%$.

In order to examine the characteristics of the phases and hardening precipitates observed in the present alloys under various heat treatment conditions, scanning electron microscopy (SEM) and field-emission scanning electron microscopy (FESEM) techniques were used. These techniques were used mainly for assessing the distribution, size, and density of the hardening precipitates in the casting structure under various aging temperatures and times as well as the alloy fracture behavior.

3. Results and Discussion

3.1. Tensile Properties. Tensile tests were carried out on all the alloys used for this study to obtain their ultimate tensile strength (UTS), yield strength (YS), and the percentage elongation (%EL) values. In addition to the as-cast condition,

TABLE 1: Chemical composition of the as-received base alloys used in this study.

| Alloy | Chemical analysis (wt.%) | | | | | | | | |
|--------|--------------------------|-------|------|-------|-------|------|------|------|---------|
| | Cu | Si | Fe | Mn | Mg | Ti | Zr | V | Al |
| HT200* | 6.5 | 0.054 | 0.05 | 0.453 | 0.006 | 0.09 | 0.18 | 0.01 | Balance |
| B319.0 | 3.3 | 5.43 | 0.42 | 0.26 | 0.27 | 0.03 | — | — | Balance |
| A356.0 | 0.12 | 7.19 | 0.12 | — | 0.32 | 0.02 | — | — | Balance |

*Chemical composition was introduced by Nematik.

TABLE 2: Chemical composition of the HT200 alloys used in this study.

| Alloy code | Chemical analysis (wt.%) | | | | | | | | | | |
|------------|--------------------------|-------|------|-------|-------|------|------|------|------|----------|-----|
| | Cu | Si | Fe | Mn | Mg | Ti | Zr | Ag | V | Sr (ppm) | Al |
| A | 6.5 | 0.054 | 0.05 | 0.453 | 0.006 | 0.09 | 0.18 | — | 0.01 | — | Bal |
| B | 6.5 | 0.054 | 0.05 | 0.453 | 0.006 | 0.13 | 0.18 | — | 0.01 | — | Bal |
| C | 6.5 | 0.054 | 0.05 | 0.453 | 0.006 | 0.15 | 0.18 | 0.50 | 0.01 | — | Bal |
| D | 3.3 | 5.43 | 0.42 | 0.26 | 0.27 | 0.12 | — | — | — | 175 | Bal |
| E | 0.12 | 7.19 | 0.12 | — | 0.32 | 0.14 | — | — | — | 160 | Bal |

the alloys were heat-treated using different heat treatment conditions, twelve in the case of alloys A, B, and C, and six in the case of alloys D and E. Before the tests were carried out, each tensile bar mounted for testing was kept in the test chamber for thirty minutes at the elevated-temperature of 250°C to stabilize the sample, after which the test was carried out. Details regarding the heat treatments used for each alloy are provided in Table 3. For each alloy/heat treatment condition, five tensile bars were tested, and the average values obtained were taken as representing the properties of that alloy/heat treatment condition.

The test bars of each alloy were divided into bundles of five, one representing the as-cast condition and the rest used for heat treatment. Six heat treatment conditions were used for this group, namely, S4A, S4W, S4WA1, S4WA2, S4WA3, and S4WA4, as described in Table 3. The alloys were solution-heat-treated at 520°C for 4 hours. For each test, the test bar was kept in the testing chamber at 250°C for 30 minutes before running the test, to ensure a homogeneous temperature distribution throughout the bar. The tensile test results for this group are plotted in Figures 1–3. The results reveal that the high-temperature tensile properties of the alloys improved significantly after heat treatment.

Heating the samples further in the testing chamber and then running the tests at 250°C coarsened the precipitates, decreased their density, increased their size, and increased the interparticle spacing so that the strength decreased and the ductility increased, when compared with the ambient temperature tensile test results. This is demonstrated visually in the micrographs shown in Figures 4 and 5, which compare the microstructures of T7-heat treated alloy B tested at ambient temperature and 250°C, respectively. It can be seen that the precipitates in Figure 5 are coarser, with greater interparticle spacing than the precipitates in Figure 4. Hence, the lower strength values obtained for this group at the elevated temperature.

In the first two heat treatment conditions, i.e., S4A and S4W (solution treatment followed by air or water

quenching), the improvement in the tensile properties is attributed to the SHT and the high cooling rate achieved with water quenching. The supersaturated solid solution obtained by the dissolution of existing phases like θ -Al₂Cu in the as-cast structure is preserved by means of rapid cooling to room temperature during the water quenching. As seen from the results for the three alloys, solution treatment with water quenching provided better tensile properties than when the bars were air quenched, due to the higher cooling rate obtained with water quenching.

Thus, following solution heat treatment and water quenching,

- (i) Alloy A exhibited 202 MPa, 134 MPa, and 6.2% for the UTS, YS, and %El, respectively (cf. 153 MPa, 88 MPa, and 6.1% in the as-cast condition)
- (ii) Alloy B had UTS, YS, and %El values of 218 MPa, 172 MPa, and 6.0% (cf. 157 MPa, 88 MPa, and 8.5% in the as-cast case), and
- (iii) Alloy C showed 223 MPa, 158 MPa, and 7.4% as its UTS, YS, and %El values (cf. 157 MPa, 103 MPa, and 5.9% in the as-cast condition)

These results may be explained based on the same reasons mentioned in the preceding paragraphs.

Aging treatment, as in the S4WA1, S4WA2, S4WA3, and S4WA4 heat treatment conditions, follows solution heat treating and quenching and is controlled by the *temperature* and *time* used. Precipitation or age hardening increases the strength in Al-Cu alloys, the main strengthening precipitates being those of the θ -Al₂Cu phase. After solution treatment and quenching, the solute atoms, which exist in the supersaturated solid solution, SSSS, start to form Guinier–Preston or GP zones. The solute atoms in these GP zones consist of ordered groups, which are coherent with the lattice structure and dispersed within the matrix. Usually these atoms have different sizes from those of the lattice structure

TABLE 3: As-cast and heat-treatment conditions and codes—shortened descriptions.

| Treatment# | As-cast and heat treatment conditions | Alloy code |
|------------|---------------------------------------|------------|
| 1 | As-cast | AC |
| 2 | SHT4_AQ | S4A |
| 3 | SHT4_WQ | S4W |
| 4 | SHT4_WQ + aging 1 | S4WA1 |
| 5 | SHT4_WQ + aging 2 | S4WA2 |
| 6 | SHT4_WQ + aging 3 | S4WA3 |
| 7 | SHT4_WQ + aging 4 | S4WA4 |
| 8 | SHT8_AQ | S8A |
| 9 | SHT8_WQ | S8W |
| 10 | SHT8_WQ + aging 1 | S8WA1 |
| 11 | SHT8_WQ + aging 2 | S8WA2 |
| 12 | SHT8_WQ + aging 3 | S8WA3 |
| 13 | SHT8_WQ + aging 4 | S8WA4 |

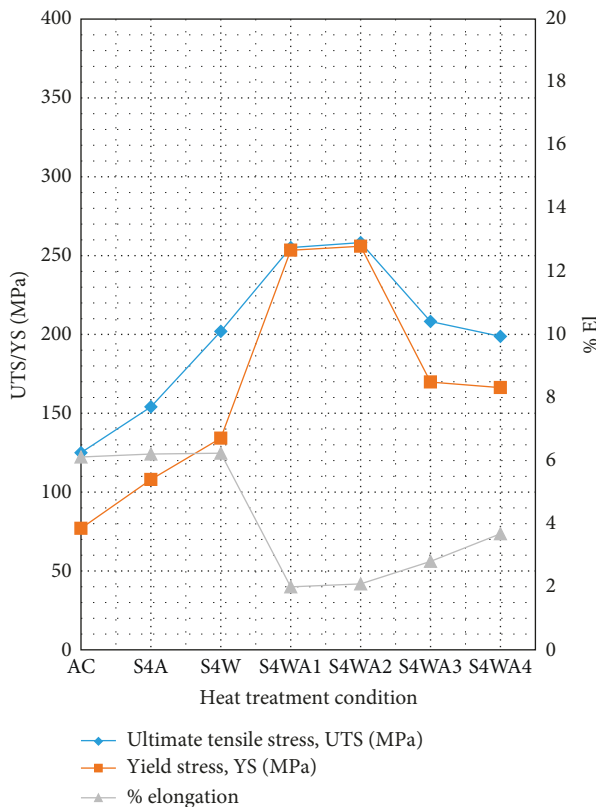


FIGURE 1: Average values of UTS, YS, %El for alloy A in the as-cast condition and after heat treatments comprising SHT for 4 h (tested at 250°C).

of the aluminum matrix; therefore, distortion occurs in the lattice, producing coherency-strain fields which lead to a significant improvement in strength [11–13].

These GP zones are metastable, and they dissolve later in the presence of a more stable phase. As the aging treatment progresses, the GP zones dissolve, and metastable coherent or semicoherent precipitates start forming. These precipitates continue to grow by diffusion of atoms from the SSSS, which results in achieving maximum or peak strength. As aging continues further, the metastable coherent

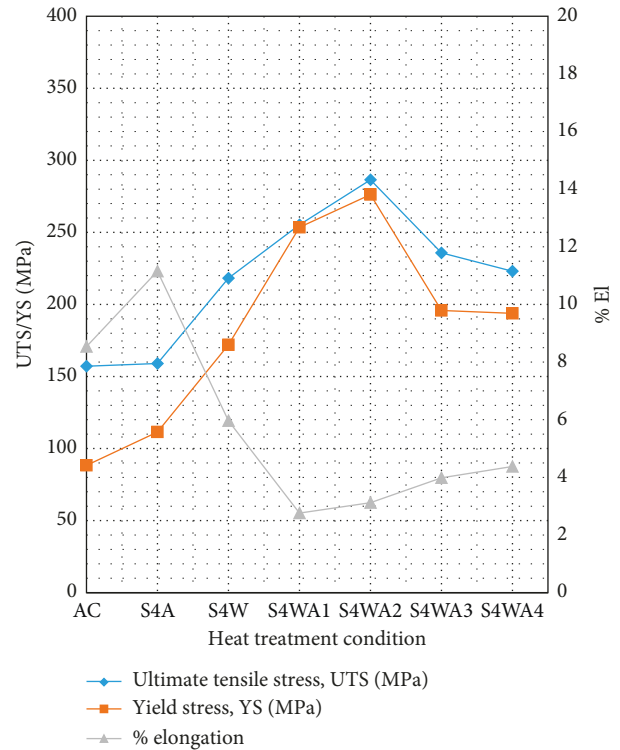


FIGURE 2: Average values of UTS, YS, %El for alloy B in the as-cast condition and after heat treatments comprising SHT for 4 h (tested at 250°C).

precipitates later become totally incoherent. In this condition, the opposition of the precipitates to dislocation movement is reduced, and this in turn leads to a consequent reduction in strength [14–16].

Peak aging is obtained when T6 heat treatment is used (S4WA1 and S4WA2), as the resulting precipitates are fine and coherent and display small interparticle spacing, which increases the opposition to dislocation motion, so that the strength is significantly increased, as can be seen in Figures 1–3:

- (i) Alloy A reached its highest strength with the S4WA2 treatment, with values of 258 MPa, 256 MPa, and 2.1% for the UTS, YS, and %El, respectively, compared to 153 MPa, 88 MPa, and 6.1% in the as-cast condition.
- (ii) Alloy B also reached its highest strength in the S4WA2 heat-treated condition, with UTS, YS, and %El values of 287 MPa, 276 MPa, and 3.1%, respectively (cf. 157 MPa, 88 MPa and 8.5% in the as-cast condition), and
- (iii) Alloy C, however, reached its highest strength after S4WA1 treatment (cf. 259 MPa, 255 MPa, and 3.2% with 157 MPa, 103 MPa, and 5.9% in the as-cast case)

The application of T7 treatment, when the aging temperature was increased as in S4WA3, or when both aging temperature and time were increased as in S4WA4, caused overaging. That is to say that the precipitates became coarse, bigger in size, lower in density, and displayed large interparticle distances. As seen from Figures 4 and 5, the

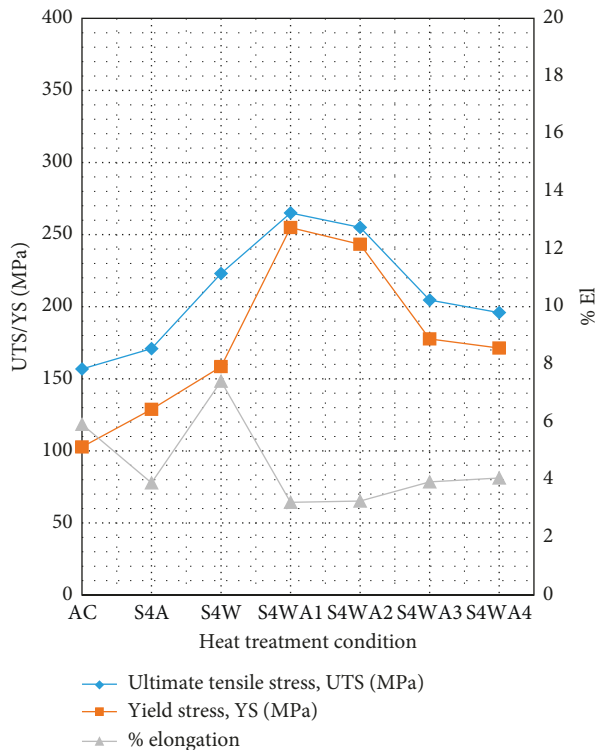


FIGURE 3: Average values of UTS, YS, %El for alloy C in the as-cast condition, and after heat treatments comprising SHT for 4 h (tested at 250°C).

precipitates in the T7 heat-treated alloy B coarsened even further, when the alloy sample was maintained at the 250°C temperature prior to testing.

The tensile properties of the alloys A, B, C, D, and E, when tested at 250°C, using test bars in the as-cast and heat-treated conditions following solution heat treatment for 8 hours, are presented in this section. Six heat treatment conditions were used in this group, namely, S8A, S8W, S8WA1, S8WA2, S8WA3, and S8WA4. Their descriptions are provided in Table 3. Alloys A, B, and C were solution-treated at 520°C for 8 hours, alloy D was solution-treated at 500°C for 8 hours, and alloy E was solution-treated at 540°C for 8 hours. Prior to testing, the test bars were kept in the testing chamber at 250°C for 30 minutes, to ensure a homogeneous temperature distribution throughout the bar before the test was carried out. The high-temperature tensile properties (UTS, YS, and %El) of alloys A, B, C, D, and E are shown in Figures 6–10.

Again, as in the case of the four hours SHT group, the results revealed that the tensile properties of alloys A, B, and C are improved upon heat treatment. The same behavior was exhibited by the reference alloys D and E when heat-treated, with improvements in the tensile properties; as shown in Figures 9 and 10. Further heating of the samples in the testing chamber and then running the tests at 250°C coarsened the precipitates, decreased their density, increased their size, and increased the interparticle spacing so that the strength decreased and the ductility increased, when compared with the ambient temperature tensile test results.

When tested at 250°C, the HT200 alloys showed lower values of strength and higher values of ductility in the as-cast condition compared to the as-cast reference alloys D and E. In the as-cast condition,

- (i) Alloy A exhibited UTS, YS, and %El values of 153 MPa, 88 MPa, and 6.1%, respectively
- (ii) Alloy B gave 157 MPa, 88 MPa, and 8.5%, while alloy C showed 157 MPa, 103 MPa, and 5.9% for the UTS, YS, and %El, respectively
- (iii) Alloy D showed 206 MPa, 153 MPa, and 3.0% for the UTS, YS, and %El, respectively, in the as-cast condition, and
- (iv) Alloy E resulted in 171 MPa, 115 MPa, and 5.8% for the UTS, YS, and %El, respectively, in the as-cast condition

Using heat treatment enhanced the mechanical properties of the HT200 alloys. Considering the first two heat treatment conditions, S8A and S8W, which comprise solution heat treatment followed by air or water quenching, it can be seen that the strength of the alloys improved. The improvement in the alloy strength is attributed to the solution heat treatment (SHT) as well as the high cooling rate that followed. As with SHT, the maximum amount of hardening solutes of Cu are retained in the solid solution in the matrix, forming a homogeneous supersaturated solid solution, SSSS, at elevated temperatures. When quenched, the SSSS formed during the solution treatment stage is preserved by means of the rapid cooling to a lower temperature, usually near the room temperature. The quenching retains the solute atoms in solution and blocks them in the positions where they got to at the high temperature during the SHT, so that the casting is ready for subsequent strengthening mechanisms [16–18].

As seen from the results for the five alloys, better tensile properties were obtained, when solution treatment was followed by water quenching than when air quenching was used, due to the higher cooling rate achieved with water quenching. Alloys D and E showed somewhat lower strength values in the S8A heat-treated condition those in the as-cast condition. This may be explained by the casting process as when the tensile bars were cast they were left to cool in the air, which caused natural aging.

In the S8W heat-treated condition,

- (i) Alloy A showed UTS, YS, and %El values of 235 MPa, 200 MPa, and 4.2%, respectively.
- (ii) Alloy B displayed 217 MPa, 152 MPa, and 4.5%, respectively.
- (iii) Alloy C exhibited 219 MPa, 198 MPa, and 4.1%, respectively.
- (iv) The reference alloy D showed 260 MPa, 188 MPa, and 5.1% as its UTS, YS and %El values, respectively.
- (v) Alloy E produced 233 MPa, 181 MPa, and 5%. The improvement in properties can be checked by comparing these results with those for the as-cast condition noted earlier in this section.

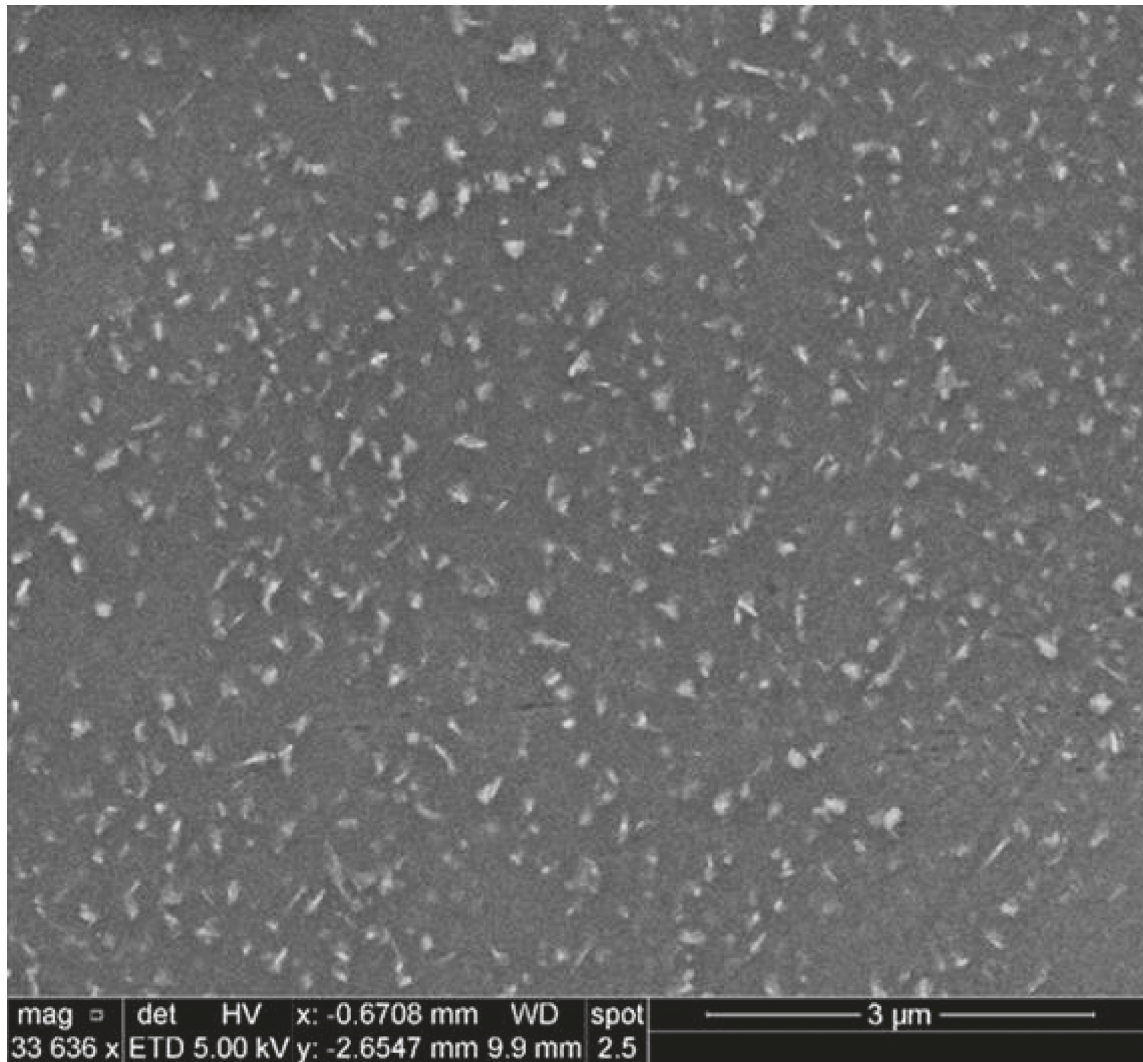


FIGURE 4: Micrograph of T7 heat-treated alloy B tested at ambient temperature.

The remainder of the heat treatments used, namely S8WA1, S8WA2, S8WA3, and S8WA4, included artificial aging, with S8WA1 and S8WA2 representing T6 heat treatments and S8WA3 and S8WA4 representing T7 heat treatments. The precipitation hardening or age hardening follows solution heat treating and quenching and is used for strengthening. Aging treatment is controlled by temperature and time. Aging increases the strength and the main hardening precipitates in Al-Cu alloys are those of the θ -Al₂Cu phase. During this aging process, the alloy reaches its peak strength and then starts to soften when the aging temperature or aging time is increased further, known as overaging; further increase in temperature may lead to annealing.

The five alloys achieved peak strength when T6 heat treatments were used (i.e., S8WA1 and S8WA2), as the precipitates were fine, coherent, and displayed small interparticle spacing; therefore, the strength increased significantly. From Figures 6–10, it can be seen that alloys A, B, and C reached their peak strength in the S8WA2 heat treatment condition. The UTS, YS, and %El values for the three alloys were 281 MPa, 280 MPa, and 2.0%; 308 MPa,

304 MPa, and 2.3%; and 276 MPa, 275 MPa, and 3.2%, respectively. From Figure 9 and 10, it can be seen that alloys D and E achieved their peak strength in the S8WA1 heat-treated condition, displaying 309 MPa, 305 MPa, and 2.8% and 283 MPa, 282 MPa, and 2.4% as their UTS, YS, and %El values, respectively. Compared to the as-cast values of each alloy, significant improvement in strength can be remarked.

When T7 treatment is used (i.e., S8WA3 and S8WA4), the strength begins to decrease and the ductility to increase, with the increase in aging temperature, which leads to overaging. In the S8WA4 heat-treatment condition, the increase in both aging temperature and aging time causes further overaging, such that the precipitates become coarser, bigger in size, and lower in density, displaying large interparticle distances as a result. This facilitates dislocation motion which in turn produces softening effects that decrease the alloy strength. Thus, in the overaged condition, the ductility of the alloy increases as its strength is decreased.

At the elevated temperature of 250°C, among the HT200 alloys, alloy B showed the highest strength values in the S8WA2 heat-treated condition with SHT for eight hours.

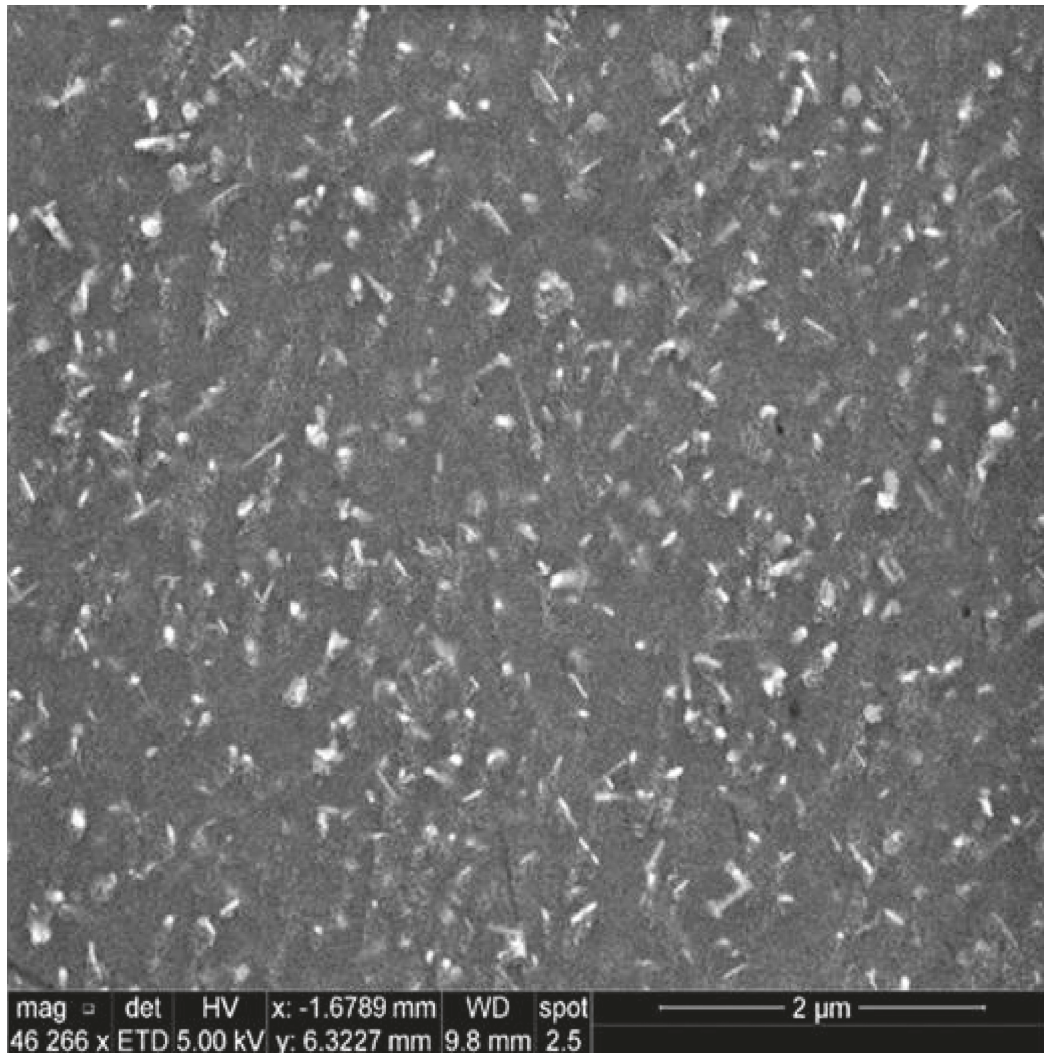


FIGURE 5: Micrograph of T7 heat-treated alloy B tested at 250°C.

Alloy B achieved competitive mechanical properties with respect to the reference alloys D and E, exhibiting UTS, YS, and %El values of 308 MPa, 304 MPa, and 2.3% (albeit at a somewhat higher aging temperature of 200°C), compared to 309 MPa, 305 MPa, and 2.8% (alloy D) and 283 MPa, 282 MPa, and 2.4% (alloy E). Alloys D and E were in the S8WA1 heat-treated condition (Table 3).

3.2. Quality Index Concept. The concept of the Quality Index (Q) was proposed by Drouzy et al. [7, 8] as a means of expressing the tensile properties of Al-Si-Mg alloys in terms of how variations in Mg content and aging conditions affected the alloy “quality” or performance. The authors used equations that allowed plotting iso-Q lines versus iso-Probable Yield Strength lines on a quality index chart, such that it became easy to see how the alloy quality was affected by the heat treatment and alloy composition [19–21]. Thus, the lines in Figures 11–13 labeled “Q” are defined as *iso-Q* lines, whereas the lines labeled “YS” are named as *iso-YS* lines, and they represent the probable yield strength.

By increasing the Cu content in aluminum alloys, the strength of the alloys can be improved significantly, although this would result in a reduction in ductility. The quality of these castings will be affected according to the net amount by which the increase in strength is balanced by the reduction in ductility. As the Q-values are a function of the ultimate tensile strength (UTS) and the percentage elongation (%El), they can thus be used as a very good indication of that balance between the strength and ductility of the alloy.

From the tensile test data shown in Figures 1–3 and Figures 6–10, quality index (Q-values) and the probable yield strength were calculated. Quality charts were then generated for evaluating the influence of the metallurgical parameters involved on the tensile properties and quality of the HT200 aluminum alloys tested at the elevated temperature, following different heat treatment conditions using SHT for four hours.

Figure 11 shows a quality chart illustrating the relationship between UTS and %El for the alloys A, B, and C in the as-cast and six heat-treatment conditions, tested at 250°C. The optimum results can be found toward the upper-

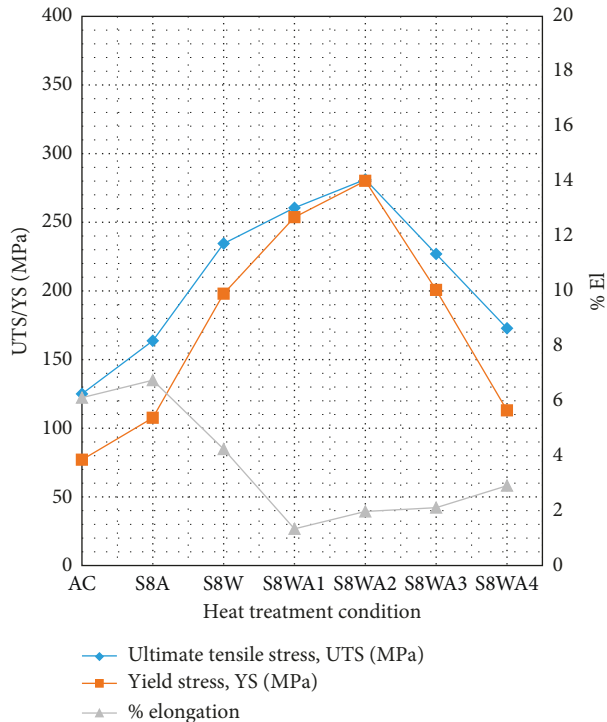


FIGURE 6: Average values of UTS, YS, and %El obtained at 250°C, for alloy A in the as-cast condition, and after heat treatments comprising SHT for 8 h.

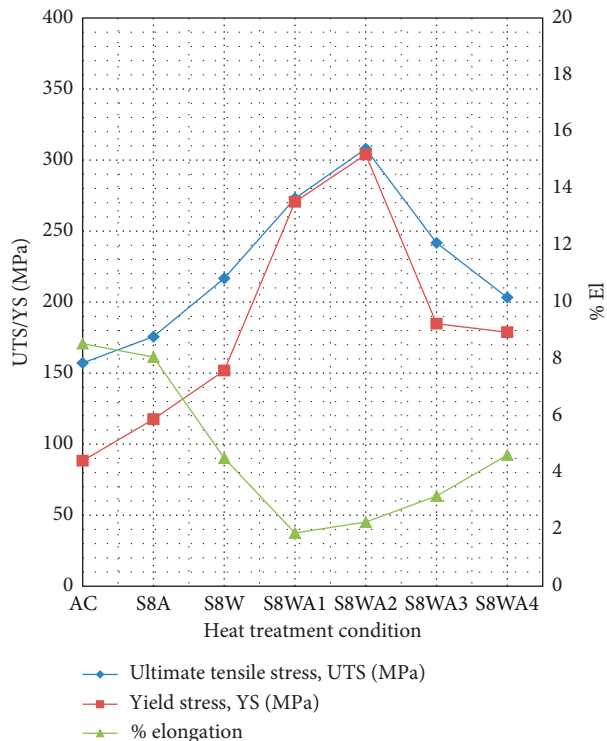


FIGURE 7: Average values of UTS, YS, and %El obtained at 250°C, for alloy B in the as-cast condition, and after heat treatments comprising SHT for 8 h.

right corner (high Q and high PYS region) of the chart. The best combination of Q and PYS values was chosen for each of the alloys following the different heat treatments, in order to determine the optimum alloy composition/heat treatment condition. Alloy A gave a Q-value of 321 MPa and a PYS value of 167 MPa in the S4W heat-treated condition and Q/PYS values of 306 MPa/252 MPa after S4WA2 heat treatment. Alloy B yielded a Q-value of 362 MPa and a PYS value of 270 MPa in the S4WA2 heat-treatment condition. Alloy C gave Q/PYS values of 353 MPa/184 MPa in the S4W heat-treated condition and 335 MPa/242 MPa after S4WA1 heat treatment. As alloy B showed much higher quality and probable yield strength values in the S4WA2 heat-treated condition than alloys A and C, the alloy B composition and the S4WA2 heat-treatment condition (T6) may be considered as the optimum alloy composition/heat-treatment condition at the elevated temperature for the HT200 alloy, for the 4-hour solution heat-treatment group.

Quality charts showing the relationship between UTS and %El are shown in Figure 12 for alloys A, B, and C, and in Figure 13 for alloys D and E. All alloys were SHT for 8 h. The points corresponding to the as-cast and six heat treatment conditions, with solution heat treatment for eight hours, are labeled in each case. The optimum results are expected to be located towards the upper-right corner (high Q and high YS region). The best combination of Q-value and PYS-value was determined for each of the alloys investigated among the different heat treatments applied, to find out the optimum alloy composition/heat treatment condition. The respective Q/YYS combinations were found to be

- (i) 329 MPa/210 MPa for alloy A in the S8W heat treated condition and 325 MPa/277 MPa after S8WA2 heat treatment
- (ii) Alloy B showed 361 MPa/300 MPa, and alloy C 352 MPa/259 MPa, also after S8WA2 treatment in both cases
- (iii) Alloys D and E (the reference alloys), displayed Q/PYS values of 376 MPa/296 MPa and 339 MPa/273 MPa, respectively, both after S8WA1 heat treatment, while alloy E exhibited Q/PYS values of 343 MPa/252 MPa following S8WA2 treatment

Quality and probable yield strength values of two heat-treatment conditions were taken for alloy A, one without aging and the other including aging to differentiate between the two heat treatment types. The Q-value for the heat treatment comprising solution heat treatment for eight hours, and no aging was slightly higher due to the higher ductility. Whereas with aging, in the T6 heat treatments, the Q-value was slightly lower and the PYS-value was significantly higher due to the higher strength resulting from aging. From the results noted above, alloy B in the S8WA2 heat-treatment condition showed higher values for Q and PYS than alloys A and C. With respect to the reference alloys, alloy B showed very comparable quality values. The highest Q-value of alloy B is very close to the highest Q-value of alloy D, while the highest PYS-value of alloy B is higher

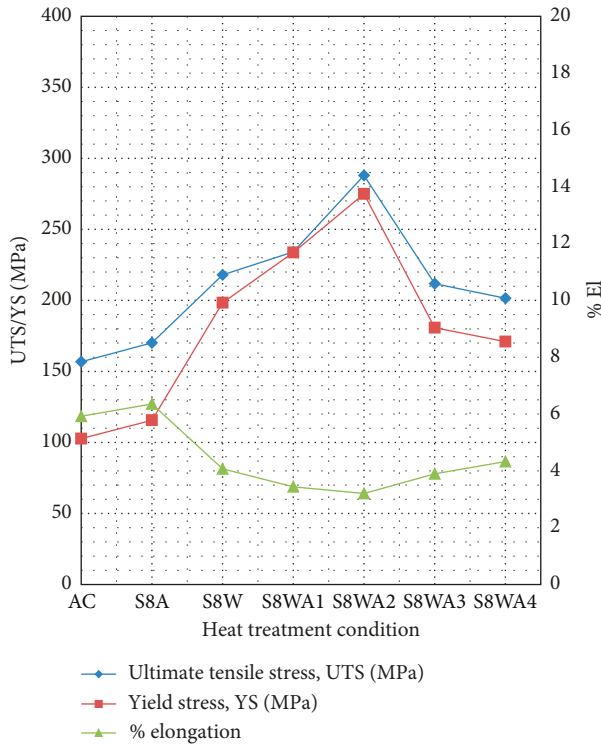


FIGURE 8: Average values of UTS, YS, and %El obtained at 250°C, for alloy C in the as-cast condition, and after heat treatments comprising SHT for 8 h.

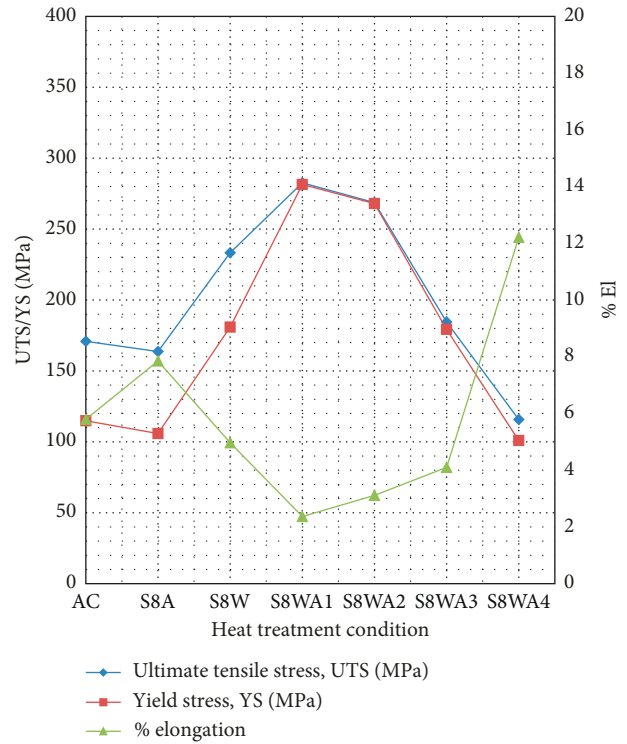


FIGURE 10: Average values of UTS, YS, and %El obtained at 250°C, for alloy E in the as-cast condition, and after heat treatments comprising SHT for 8 h.

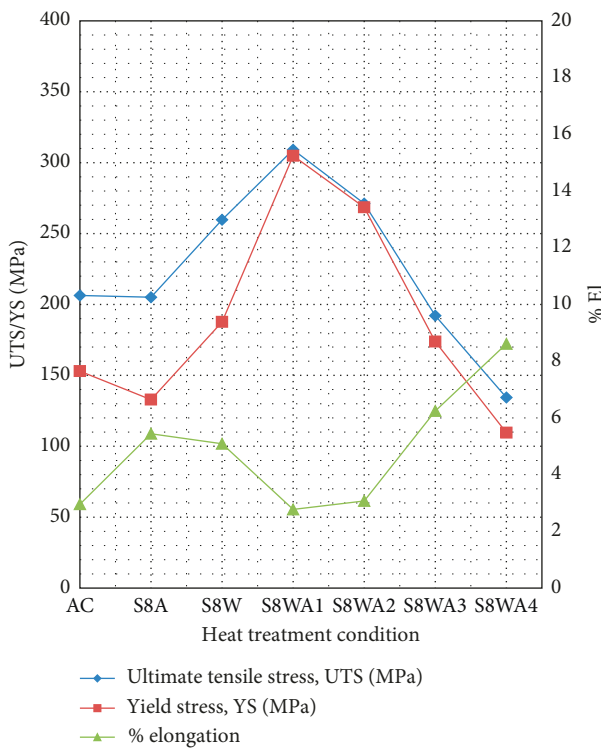


FIGURE 9: Average values of UTS, YS, and %El obtained at 250°C, for alloy D in the as-cast condition, and after heat treatments comprising SHT for 8 h.

than the highest PYS-value of the same alloy. In comparing the Q- and PYS-values of alloy B with alloy E, alloy B gave higher results.

By comparing the Q/PYS results of alloy B in the T6 heat-treated condition S4WA2 with solution heat treatment for four hours (361 MPa/270 MPa), with those of alloy B in the T6 heat-treatment condition S8WA2 but with solution heat treatment for eight hours (361 MPa/300 MPa), it can be concluded that alloy B in the S8WA2 condition corresponds to the optimum alloy composition/heat treatment condition for the HT200 alloy at the elevated temperature.

Figure 14 presents a panel chart showing the Q-values for each of the five alloys A, B, C, D, and E in the as-cast condition, and following the 12 heat treatment conditions (six with solution heat treatment times of 4 h and six with SHT times of 8 h), obtained from the tests carried out at 250°C. On an individual basis, alloy B gives the most consistent quality across the range of heat treatments used. The maintenance in strength may be attributed to the Zr which would form precipitates that retain their strength at high temperature, while the Q-values of the five alloys vary on going from the as-cast condition through all the heat treatment conditions used in this study. The reference alloy D or 319 alloy exhibits higher quality than the other alloys after 8 hours of solution treatment followed by water quenching, up until an aging temperature of 180°C (S8WA1 treatment). At higher aging temperatures, the alloy quality decreases rapidly as the alloy softens, with alloy B showing a better quality than the other alloys at these temperatures,

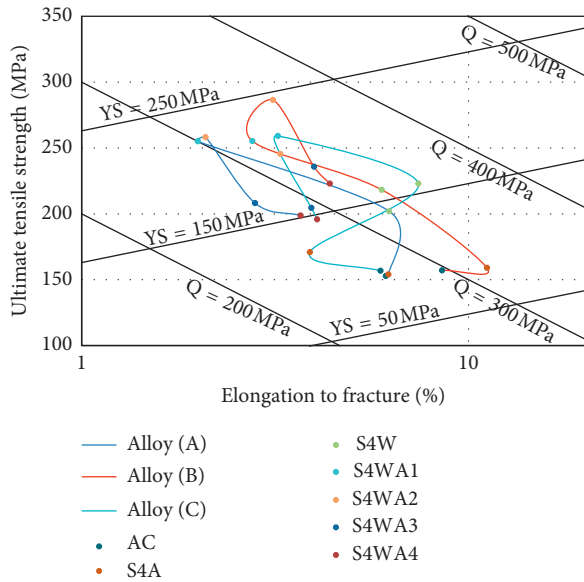


FIGURE 11: Quality chart showing relationship between UTS and % El for the A B and C alloys in the as-cast and six heat treatment conditions with SHT for 4 h.

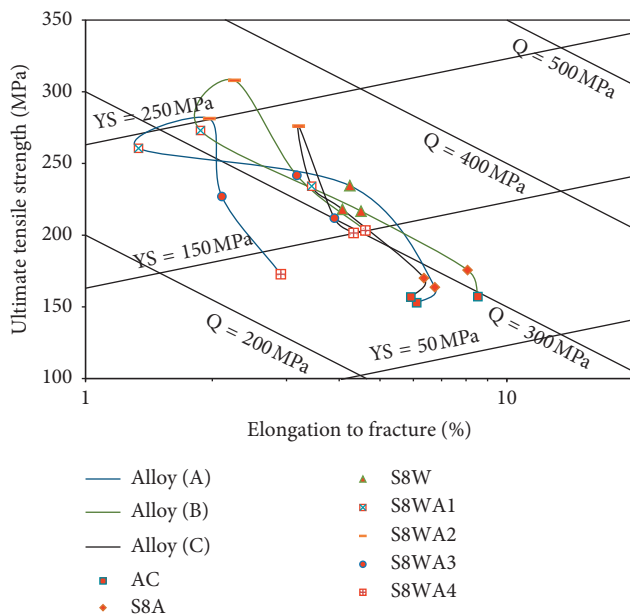


FIGURE 12: Quality chart showing relationship between UTS and % El for the A B and C alloys in the as-cast and six heat treatment conditions with SHT for 8 h.

again attributed to a retention of its strength due to the presence of Zr.

3.3. Statistical Analysis. This section presents a comparison of the tensile properties (UTS, YS, and %El) of the different alloys under different heat treatment conditions, following solution heat treatment for four and eight hours, with those of the base alloy A in the as-cast condition, for tests carried out at 250°C. Figure 15 depicts the tensile properties

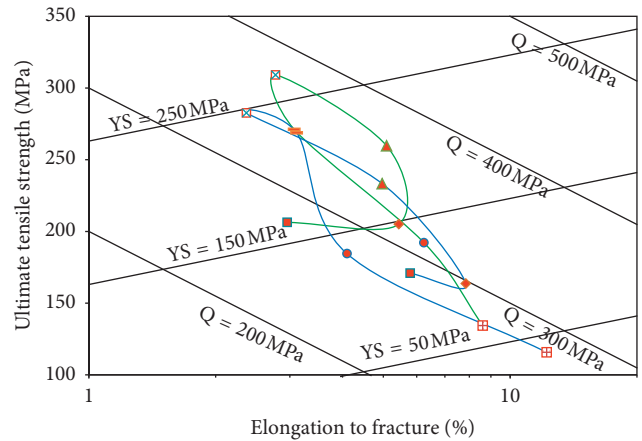


FIGURE 13: Quality chart showing relationship between UTS and % El for the D and E alloys in the as-cast and six heat treatment conditions with SHT for 8 h.

obtained for Alloys A, B, and C for these different heat-treatment conditions, relative to the values obtained for the base alloy A in the as-cast condition, i.e., after subtracting the values obtained for the base alloy A for each condition, and plotted as ΔP values on the y-axis ($P = \text{Property} = \text{UTS, YS or \%El}$), with the x-axis representing the base line for alloy A. The numbers on the x-axis represent the as-cast condition and the different heat treatment conditions used. These conditions are indicated by numbers to facilitate reading the data. Each of the numbers with the conditions they refer to is provided in Table 3.

Regarding alloys A, B, and C, it may be seen from Figure 15 that their mechanical properties were generally enhanced. The strength of the base alloy A improved by as much as 70–130 MPa with some of the aging treatments applied, namely, S8WA1, S8WA2, and S8WA3, while the ductility showed a corresponding decrease. Highest strengths were displayed by alloy B, due to the addition of the grain refiners (Ti and Zr), as well as the heat treatments applied, particularly in the case of the S8WA1 and S8WA2 treatments. With respect to alloys B and A, the improvements observed for alloy C for these treatments were slightly lower. As Figure 15(c) shows how the much higher strengths achieved with heat treatment are reflected in the corresponding low ductility values exhibited in each case, except for the S8A condition (solution treatment + air quenching) which exhibited the lowest gain in strength.

Compared to the as-cast HT200 base alloy A, the reference alloys D and E display better as-cast strength, as seen in Figures 15(a) and 15(b). The strength of the alloys improved with heat treatment, particularly with S8WA1 and S8WA2 T6 treatments, alloy D showing higher improvements, in general, and correspondingly, lower ductility values compared to alloy E. Considerable softening of the alloy was observed when the aging temperature and time were highest, i.e., 250°C and 100 hours when the S8WA4

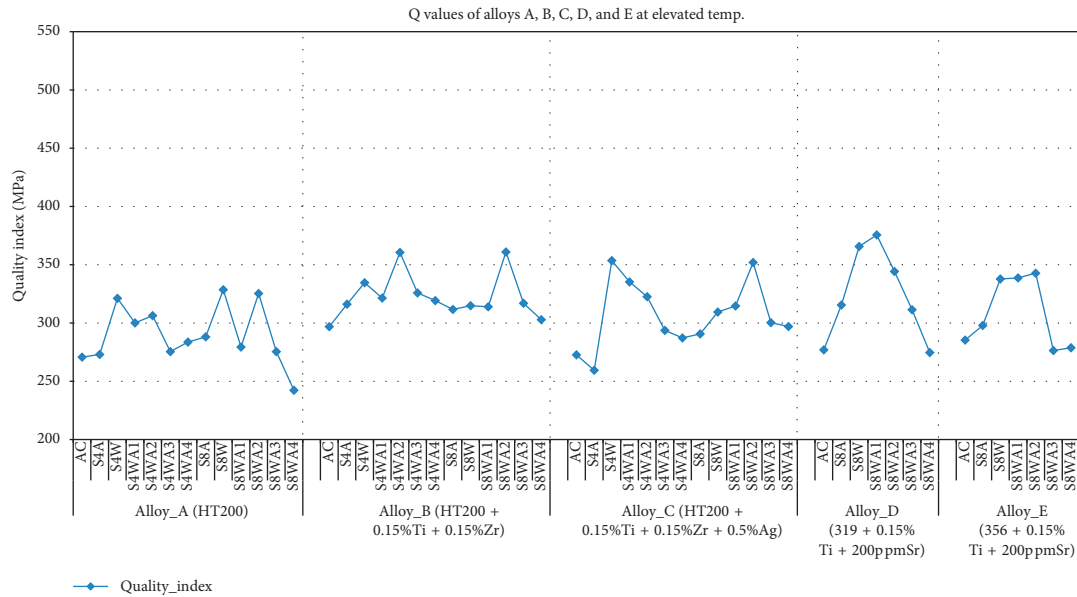


FIGURE 14: A panel chart for the quality values of alloys A, B, C, D, and E in the as-cast condition and the 12 heat-treatment conditions used in this study.

treatment was applied, the UTS reaching values lower than the as-cast HT200 base alloy. It must be borne in mind that the effects of temperature were further emphasized by the high-temperature testing conditions.

Comparison of the tensile properties of the five alloys A, B, C, D, and E with those of the as-received base alloy A is shown in Figure 15 as well. At the elevated testing temperature, the as-received HT200 alloy (alloy A) showed lower tensile properties (UTS, YS, and %El) with respect to the reference alloys D and E in the as-cast and solution heat-treated conditions (with SHT for eight hours). This is attributed to the 7% Si content of the 319 and 356 alloys which would provide a significant contribution to the strength, particularly after solution treatment, compared to the HT200 alloy. On the other hand, the higher strength values exhibited by the HT200 alloys compared to the B319.0 and A356.0 alloys after peak aging has been achieved show the advantage of the Zr addition in maintaining the alloy resistance to softening at high temperatures.

In addition, Figure 15 reveals that compared to the HT200 alloys, the reference alloys B319.0 and A356.0 show higher strength values in the as-cast condition and following 8 hours solution heat treatment, as well as in the T6 condition. The higher strength in their case is attributed to the silicon content of the alloys which provides an added contribution to the strength besides that of the precipitates. Coarsening of these constituents in the T7 condition and the additional exposure to temperature at the elevated temperature testing conditions results in the increase in ductility values observed for the 319 and 356 alloys condition #13 in Figure 15(c).

3.4. Fractography. The purpose of fractography is to analyze fracture features and attempt to relate the topography of the fracture surface to the causes and/or basic mechanisms of

fracture; the knowledge of fracture behavior is important in upgrading material specifications, improving product design, and analyzing failures for improved reliability. A study of the characteristics of fracture surfaces is often carried out using optical microscopy (viz., light-microscope fractography), particularly when a low magnification of the fracture surface is adequate. The magnification is usually selected so that a good resolution is obtained and can range from “macroscopic” or low-magnification fields (up to 50 diameters) to “microscopic” or high-magnification fields (50 diameters and above) [22].

In the present section, the fracture of Al-Cu alloys (represented by alloy B) and Al-Si-Cu alloys (represented by alloy D) and Al-Si alloys (represented by alloy E) will be examined. The tensile bars were artificially aged at 250°C for a 100 h (stabilization treatment) prior to resting at 250°C. Figure 16(a) demonstrates the effect of heat treatment on the fracture behavior of alloy B. Following stabilization treatment, the fracture surface reveals a uniform coarse dimple structure with no visible intermetallics. The dimples are seen to be stretched in the tensile testing direction (normal to the fracture surface). A high-magnification image of the fracture surface of alloy B is shown in Figure 16(b), exhibiting the depth of the dimples in Figure 16(a) due to the high alloy ductility, with slip marks on their interior surfaces (white arrows). Following pulling of the tensile bars to fracture at 250°C, the fracture surface in Figure 16(c) clearly reflects the increase in the alloy % elongation as inferred from the increase in both size and depth of the dimple structure compared to that presented in Figure 16(a). The white circles in Figure 16(c) display the precipitation of coarse Al₂Cu phase particles (approximately 300–500 μm in size).

The fracture surface of alloy D tested at 250°C is illustrated in Figure 17(a) showing the fracture of the brittle β-Fe intermetallic phase as confirmed from the associated EDS spectrum presented in Figure 17(b). In addition, dense

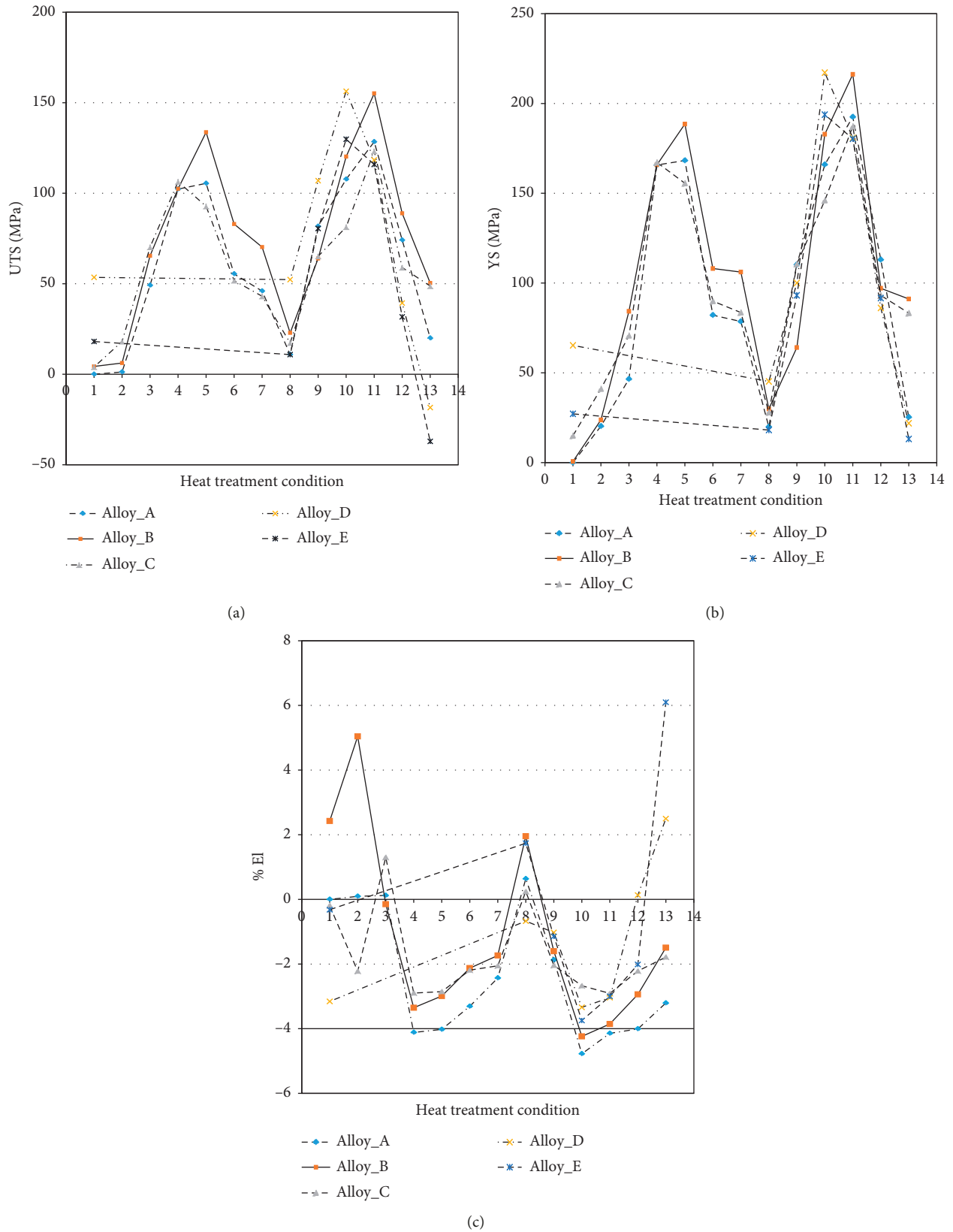


FIGURE 15: Comparison of tensile properties of A, B, C, D, and E alloys relative to those of as-cast base alloy A (a) ΔP -UTS, (b) ΔP -YS, and (c) ΔP -%EI as a function of heat-treatment conditions with SHT for 4 h and 8 h.

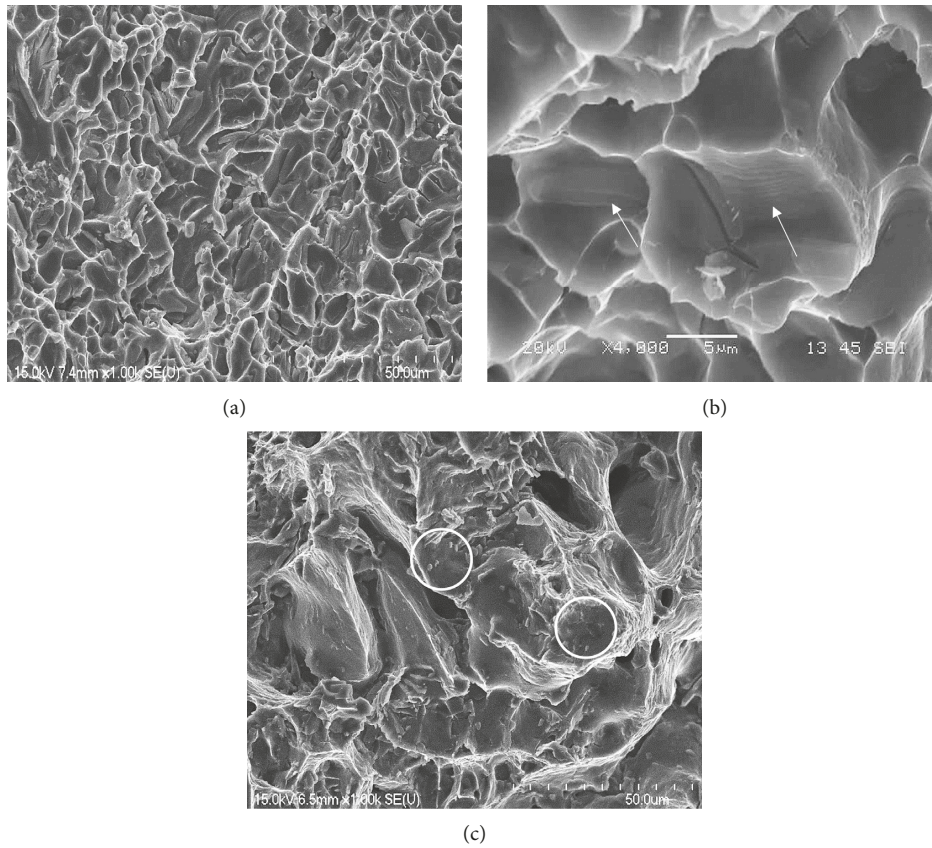


FIGURE 16: Secondary electron micrographs of the fracture surface of alloy B (a) after stabilization treatment (tested at 25°C), (b) a high magnification of (a), and (c) after testing at 250°C.

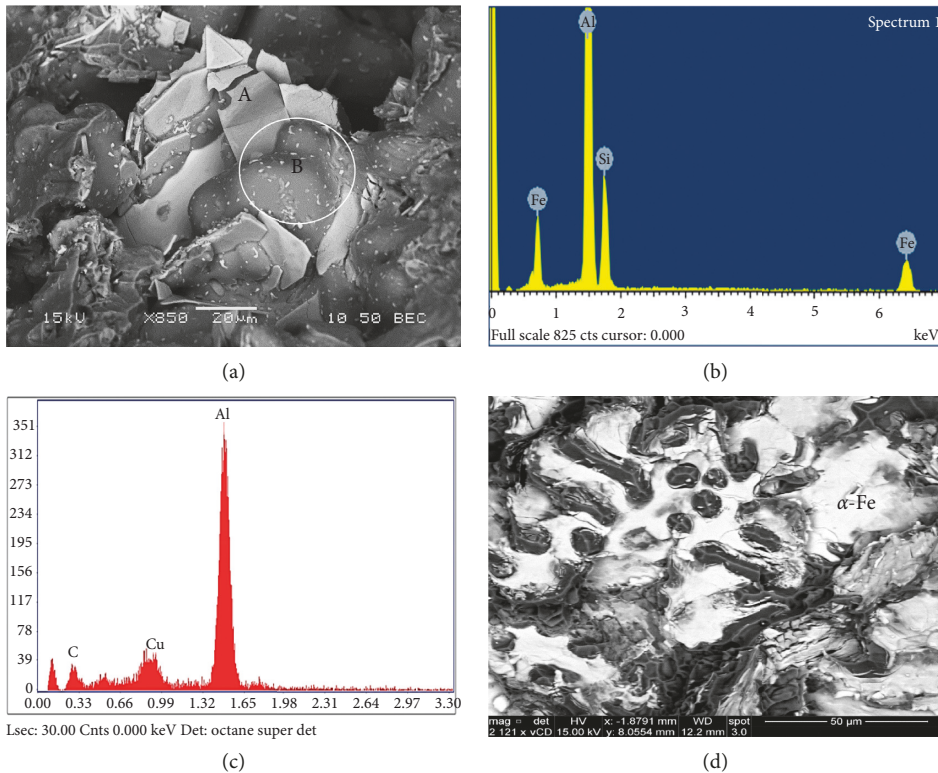


FIGURE 17: Backscattered electron micrographs of the fracture surface of alloys D and E following stabilization treated prior to testing at 250°C: (a) alloy D; (b) EDS spectrum corresponding to β -Fe platelets in (a) marked A; (c) EDS spectrum of Al_2Cu particles in (a) marked B; (d) alloy E.

TABLE 4: Optimum high-temperature tensile properties and Q values for the alloys studied.

| Alloy | Optimum tensile properties | | | Q-value (MPa) | Heat treatment condition |
|-------|----------------------------|----------|--------|---------------|--------------------------|
| | UTS (MPa) | YS (MPa) | (%) El | | |
| A | 281 | 280 | 2.0 | 325.3 | S8WA2 |
| B | 308 | 304 | 2.3 | 361.0 | S8WA2 |
| C | 276 | 275 | 3.2 | 351.9 | S8WA2 |
| D | 309 | 305 | 2.8 | 375.6 | S8WA1 |
| E | 283 | 282 | 2.4 | 338.7 | S8WA1 |

precipitation of Al₂Cu phase particles marked B are seen covering the dendrites (viewed within a pore). Due to the nanosize of the Al₂Cu precipitates, the Cu peak in the EDS spectrum shown in Figure 17(c) appears at about 0.8 eV corresponding to the L1 line. Farhadi et al. [23] reported on the effect of Sr and annealing on the fragmentation of α -Fe in 5xxx alloys. Figure 17(d) exhibits the fracture surface of alloy E (modified with 200 ppm Sr) where a large α -Fe phase particle is seen to be perforated due to its destabilization caused by Sr modification which minimizes its harmful effect on the alloy tensile properties.

4. Conclusions

Based on the results obtained from the present study, the following conclusions may be drawn:

Design engineers usually design components using the YS of the alloy selected. Therefore, the higher YS of one of the alloys at one of the heat treatment options is significant (Table 4).

- (1) Optimum high-temperature tensile properties (YS) and Q-values for the five alloys investigated and the corresponding heat treatment conditions which provided these properties are summarized in the Table 4 below
- (2) The best strength results were obtained when aging was carried out. T6 heat treatments gave higher strength than T7 heat treatments, where overaging and alloy softening commenced
- (3) Alloy B gives the best overall performance among the range of heat treatments employed with respect to the HT200 alloys, with properties comparable to the widely used B319.0 and A356.0 reference alloys
- (4) The presence of Ag in alloy C enhanced the YS of alloy A by ~17% in the as-cast condition and also showed a slight improvement in UTS, going from 153 MPa to 157 MPa

Data Availability

The data used to support the findings of this study are available from the corresponding author upon request.

Conflicts of Interest

The authors declare that they have no conflicts of interest.

Acknowledgments

The authors would like to thank Amal Samuel for enhancing the quality of the artwork used in the present article.

References

- [1] L. Bäckerud, G. Chai, and J. Tamminen, *Solidification Characteristics of Aluminum Alloys Volume 2: Foundry Alloys*, American Foundrymen's Society/Skanaluminium, Schaumburg, IL, USA, 1990.
- [2] E. M. Elgallad, *Effect of additives on the mechanical properties and machinability of a new aluminum-copper base alloy*, Ph.D. thesis, Université du Québec à Chicoutimi, Chicoutimi, Canada, 2010.
- [3] G. E. Totten and D. S. MacKenzie, *Handbook of Aluminum Volume 1—Physical Metallurgy and Processes*, Marcel Dekker, New York, NY, USA, 2003.
- [4] H. K. Kamga, *Influence of alloying elements iron and silicon on mechanical properties of aluminum-copper type B206 alloys*, Ph.D. thesis, Université du Québec à Chicoutimi, Chicoutimi, Canada, 2010.
- [5] D. H. Xiao, J. N. Wang, D. Y. Ding, and S. P. Chen, "Effect of Cu content on the mechanical properties of an Al-Cu-Mg-Ag alloy," *Journal of Alloys and Compounds*, vol. 343, no. 1-2, pp. 77-81, 2002.
- [6] R. Mahmudi, P. Sepehrband, and H. M. Ghasemi, "Improved properties of A319 aluminum casting alloy modified with Zr," *Materials Letters*, vol. 60, no. 21-22, pp. 2606-2610, 2006.
- [7] M. Drouzy, S. Jacob, and M. Richard, "Interpretation of tensile results by means of quality index and probable yield strength," *AFS International Cast Metals Journal*, vol. 5, pp. 43-50, 1980.
- [8] M. Drouzy, S. Jacob, and M. Richard, "L'Indice de Qualité et la Limite d'élasticité des Alliages A-S7 G," *Fonderie*, vol. 360, pp. 345-349, 1975.
- [9] M. Drouzy, S. Jacob, and M. Richard, "Le diagramme charge de rupture allongement des Alliages d'aluminium: l'indice de qualité—application aux A-S7 G," *Fonderie*, vol. 355, pp. 139-147, 1976.
- [10] A. Girgis, M. H. Abdelaziz, A. M. Samuel, S. Valtierra, and F. H. Samuel, "On the enhancement of the microstructure and tensile properties of an Al-Cu based cast alloy," *Metallography, Microstructure, and Analysis*, vol. 8, no. 5, pp. 757-769, 2019.
- [11] A. K. Gupta, D. J. Lloyd, and S. A. Court, "Precipitation hardening in Al-Mg-Si alloys with and without excess Si," *Materials Science and Engineering: A*, vol. 316, no. 1-2, pp. 11-17, 2001.
- [12] Y. Aruga, S. Kim, M. Kozuka, E. Kobayashi, and T. Sato, "Effects of cluster characteristics on two-step aging behavior in Al-Mg-Si alloys with different Mg/Si ratios and natural aging periods," *Materials Science and Engineering: A*, vol. 718, pp. 371-376, 2018.
- [13] Y. Aruga, M. Kozuka, and T. Sato, "Formulation of initial artificial age-hardening response in an Al-Mg-Si alloy based on the cluster classification using a high-detection-efficiency atom probe," *Journal of Alloys and Compounds*, vol. 739, pp. 1115-1123, 2018.
- [14] Y. Aruga, M. Kozuka, Y. Takaki, and T. Sato, "Effects of natural aging after pre-aging on clustering and bake-hardening behavior in an Al-Mg-Si alloy," *Scripta Materialia*, vol. 116, pp. 82-86, 2016.

- [15] L. Ding, Z. Jia, Y. Liu, Y. Weng, and Q. Liu, "The influence of Cu addition and pre-straining on the natural aging and bake hardening response of Al-Mg-Si alloys," *Journal of Alloys and Compounds*, vol. 688, pp. 362–367, 2016.
- [16] S. Jin, T. Ngai, L. Li, Y. Lai, Z. Chen, and A. Wang, "Influence of natural aging and pre-treatment on the precipitation and age-hardening behavior of Al-1.0 Mg-0.65 Si-0.24 Cu alloy," *Journal of Alloys and Compounds*, vol. 742, pp. 852–859, 2018.
- [17] F. J. Tavitas-Medrano, A. M. A. Mohamed, J. E. Gruzleski, F. H. Samuel, and H. W. Doty, "Precipitation-hardening in cast Al-Si-Cu-Mg alloys," *Journal of Materials Science*, vol. 45, no. 3, pp. 641–651, 2010.
- [18] F. J. Tavitas-Medrano, S. Valtierra, J. E. Gruzleski, F. H. Samuel, and H. W. Doty, "A TEM study of the aging behavior of 319 type alloys," in *Proceedings of the Transactions of the American Foundry Society: 112th Metalcasting Congress*, pp. 99–114, American Foundry Society, Atlanta, GA, USA, May 2008.
- [19] H. R. Ammar, A. M. Samuel, F. H. Samuel, and A. M. A. Al-Ahmari, "Aging behavior of 359-type Al-9% Si-0.5% Mg casting alloys," *Journal of Materials Science*, vol. 47, no. 3, pp. 1331–1338, 2012.
- [20] H. R. Ammar, C. Moreau, A. M. Samuel, F. H. Samuel, and H. W. Doty, "Effects of aging parameters on the quality of 413-type commercial alloys," *Materials & Design*, vol. 30, no. 4, pp. 1014–1025, 2009.
- [21] J. Hernandez-Sandoval, G. H. Garza-Elizondo, A. M. Samuel, S. Valtierra, and F. H. Samuel, "The ambient and high temperature deformation behavior of Al-Si-Cu-Mg alloy with minor Ti, Zr, Ni additions," *Materials & Design*, vol. 58, pp. 89–101, 2014.
- [22] Z. Ma, A. M. Samuel, H. W. Doty, and F. H. Samuel, *On the Fractography of Impact-Tested Samples of Al-Si Alloys for Automotive Alloys*, Intech Publications, Rijeka, Croatia, 2016.
- [23] G. A. Farhadi, A. M. Samuel, F. H. Samuel, H. W. Doty, and B. Kulunk, "Alloy performance in relation to intermetallic fragmentation observed in 5XXX aluminum alloys in the Sr-modified and annealed conditions in light metals 2000—métaux légers," in *Proceedings of the International Symposium on Light Metals*, J. Kazadi and J. Masounave, Eds., pp. 71–94, Canadian Institute of Mining, Metallurgy and Petroleum, Ottawa, Canada, August 2000.



Hindawi
Submit your manuscripts at
www.hindawi.com

